Biophysical Chemistry 27 (1987) 27–38
Elsevier

BPC 01130

Rotational modes of Ca^{2+}-liganded calmodulin, as determined by time-domain fluorescence

Robert F. Steiner and Lynn Norris

Department of Chemistry, University of Maryland (Baltimore County), Catonsville, MD 21228, U.S.A.

Received 20 August 1986
Accepted 14 January 1987

Calmodulin; Ca^{2+}; Fluorescence anisotropy; Time-domain fluorescence

The time decay of fluorescence anisotropy was monitored as a function of pH and temperature for complexes of 2,6-toluidinylnaphthalenesulfonate with calmodulin, with its proteolytic fragments, and with the 1:1 complex of calmodulin and melittin. For all the conditions examined the anisotropy decay of native calmodulin involved at least two rotational modes. These corresponded to a short correlation time of 2–3 ns, reflecting a localized motion in the vicinity of the binding site and a longer correlation time which arises from the rotation of a major portion of the molecule. The relative amplitudes of the two rotational modes were dependent upon temperature in the range 11–40°C, the contribution of the more rapid mode increasing with temperature. The maximum immobilization of the probe occurred at pH 5.0 and 12°C. While these results indicate the presence of internal rotations in Ca^{2+}-liganded calmodulin, the magnitude of the longer correlation time is consistent with the crystallographic structure.

1. Introduction

Calmodulin, a Ca^{2+}-binding protein ubiquitous in eukaryotic systems, has been shown to combine with, and regulate the activities of, a large number of diverse enzymes [1–3]. The combination with the regulated enzyme is generally Ca^{2+}-dependent [1–3]. Calmodulin is probably the most important initial receptor for biological signals involving a change in the level of Ca^{2+} [1–3].

The major unresolved questions concerning the activity of calmodulin include the origins of its unusual versatility of function, which enables it to combine with enzymes of very different structures and properties. It has been suggested that some form of molecular adaptability, or flexibility, may be a factor in the properties of calmodulin [1,4].

The three-dimensional crystallographic structure of the Ca^{2+}-liganded form of calmodulin has recently been announced [5]. It is roughly dumbbell-shaped, consisting of two globular lobes joined by an extended α-helical strand (residues 66–92). The N-terminal lobe contains the two weaker Ca^{2+}-binding sites I and II, while the C-terminal lobe contains the two stronger sites III and IV. The molecule as a whole is rather asymmetric, being about 65 Å long, while the two globular N- and C-terminal lobes each have dimensions of about $20 \times 20 \times 25$ Å [5].

The crystallographic structure determination was carried out for calmodulin which had been crystallized from an acid medium (50 mM cacodylate, pH 5.6, 4 mM $CaCl_2$) [5]. A question remains as to what extent the connecting strand retains its helical character in solution, especially in the absence of Ca^{2+}.

Correspondence address: R.F. Steiner, Department of Chemistry, University of Maryland (Baltimore County), Catonsville, MD 21228, U.S.A.

Abbreviations: TNS, 2,6-toluidinylnaphthalenesulfonate; HPLC, high-performance liquid chromatography; Mops, 3-(*N*-morpholino)propanesulfonate; CaM, calmodulin, ME, melittin.

This paper will present time-domain measurements of fluorescence anisotropy decay for Ca^{2+}-liganded calmodulin and its proteolytic fragments under varying conditions of pH, ionic strength, and temperature, with the objectives of completing and extending earlier studies upon the molecular dynamics of calmodulin and of comparing the observed behavior with that expected for the intact crystallographic structure [6,7]. It is of interest to characterize any internal rotational modes and to establish their dependence upon conditions. These studies have taken advantage of recent advances in instrumentation and data analysis.

The fluorophore employed in this investigation was TNS, which is almost non-fluorescent in aqueous solution, but which undergoes a Ca^{2+}-dependent combination with calmodulin to yield a strongly fluorescent complex [8]. The use of TNS had the advantage of minimizing the contribution of rotation confined to the fluorescent label, in view of its probable contact with several amino acid side chains on the protein surface.

Calmodulin contains two binding sites for TNS; the N-terminal (1–77) and C-terminal (78–148) half-molecules each containing a binding site [9,10]. The interaction is Ca^{2+}-dependent, little or no binding occurring for the apoprotein. The location of the sites is uncertain. If they are equivalent to, or overlap, those for trifluoperazine, which also combines in a Ca^{2+}-dependent manner, a feasible location is on the connecting bridge, near the junctions with the N- and C-terminal lobes [11].

The basic questions to be asked in this study are:

(i) Can the time decay of fluorescence anisotropy for Ca^{2+}-liganded calmodulin be interpreted in terms of the crystallographic structure?

(ii) Do internal rotational modes exist and, if so, how do they depend upon external conditions?

2. Experimental

2.1. Materials

Calmodulin was isolated from bovine testes (Pel-Freez) by the method of Watterson et al. [12]. The product was homogeneous by the criterion of SDS-acrylamide gel electrophoresis and its amino acid composition corresponded to the expected values.

The half-molecules TR_1C (1–77) and TR_2C (78–148) were obtained by tryptic digestion in the presence of Ca^{2+}, according to the procedure of Brzeska et al. [13]. The fragments were separated by reverse-phase HPLC using a C-18 column and the elution procedure of Guerini et al. [14]. They were further purified by HPLC as described by Newton et al. [15]. The amino acid compositions of the products corresponded closely to the expected values.

The fragments TM_1 (1–106) and TM_2 (107–148) were prepared by thrombin digestion of calmodulin, as described by Guerini et al. [14]. They were separated and further purified by reverse-phase HPLC according to the procedures of Guerini et al. [14]. Their amino acid compositions corresponded closely to the predicted values.

Thrombin and trypsin (TPCK) were purchased from Sigma, as was TNS. All other chemicals were reagent grade, or better.

Amino acid analyses were performed by Dr. Lou Henderson.

2.2. Methods

The time decays of fluorescence intensity and anisotropy were measured using an Edinburgh nanosecond fluorometer located in the laboratory of Dr. J.R. Lakowicz in the Department of Biological Chemistry, School of Medicine, University of Maryland (Baltimore). This instrument utilizes a gas-filled lamp as pulser; for these studies N_2 at a pressure of 1.5 bar was used. The flashing frequency of the lamp was 30 kHz. The excitation beam was vertically polarized. The excitation wavelength was 360.7 nm; a Corning 3–73 cut-off filter intercepted the fluorescence beam. With this filter combination, virtually the entire emission band was observed, while the background was less than 1%. A Ludox silica suspension was used as a scattering solution to monitor the time profile of the excitation pulse, thereby providing the instrumental response function $P(t)$. The analyzer was automatically shifted between vertical and horizontal positions in 1-min cycles for periods of 2–3 h.

The time-dependent fluorescence intensity, $S(t)$, is given by eq. 1, for vertically polarized exciting light:

$$S(t) = \mathrm{VV} + 2g\mathrm{VH} \tag{1}$$

where VV and VH are the intensities of the vertically and horizontally polarized components, respectively, of fluorescence excited by vertically polarized light and $g = \mathrm{HV}/\mathrm{HH}$, where HV and HH are the vertically and horizontally polarized components, respectively, of fluorescence excited by horizontally polarized light.

The time decay of fluorescence intensity, $S(t)$ was represented by a model of the form:

$$S(t) = \sum_i \alpha_i e^{-t/\tau_i} \tag{2}$$

where α_i and τ_i are the amplitude and decay time, respectively of the i-th decay component and t is the time. The determination of the values of the α_i and τ_i from the experimental data was done using the least-squares fitting programs FIT2 and FIT3 supplied by the manufacturer (Edinburgh). These programs utilize trial values of the τ_i to generate the intensity decay function $S(t)$. The computed curve of $S(t)$ is convolved with the instrumental response function $P(t)$ to yield a computed intensity decay function $S_{\mathrm{com}}(t)$. This is compared with the experimental decay function $S_{\mathrm{exp}}(t)$ and a value of χ^2 is calculated. χ^2, the criterion for goodness of fit, is given by

$$\chi^2 = \sum_i \left\{ \frac{S_{\mathrm{exp}}(j) - S_{\mathrm{com}}(j)}{\rho(j)} \right\}^2 \tag{3}$$

where $S_{\mathrm{exp}}(j)$ and $S_{\mathrm{com}}(j)$ are the values of $S_{\mathrm{exp}}(t)$ and $S_{\mathrm{com}}(t)$ for the j-th data point and $\rho(j)$ is the corresponding precision. For intensity decay data, $\rho(j)$ is equal to $\sqrt{Y(j)}$, where $Y(j)$ is the number of single photon counts for the j-th point.

The set of values of the τ_i which correspond to a minimum value of χ^2 are located by an iterative procedure in which each τ_i is incremented until χ^2 passes through a minimum. The value of τ_i corresponding to a minimal value of χ^2 is identified by a parabolic interpolation. This is done for each of the τ_i in turn until the overall optimum fit is attained. For each set of values of the τ_i the optimum values of the α_i are obtained by a linear least-squares fit.

The time-dependent fluorescence anisotropy, $A(t)$ is given by:

$$A(t) = \frac{\mathrm{VV} - g\mathrm{VH}}{\mathrm{VV} + 2g\mathrm{VH}} = D(t)/S(t) \tag{4}$$

where $D(t) = \mathrm{VV} - g\mathrm{VH}$

The time decay of anisotropy is represented by a model of the form:

$$A(t) = \sum_i \beta_i e^{-t/\sigma_i} + A(\infty) \tag{5}$$

where β_i and σ_i are the amplitude and rotational correlation time, respectively, corresponding to the i-th rotational mode and $A(\infty)$ is the limiting value of the anisotropy at very long times after excitation. For fluorescent molecules which are not partially, or wholly, immobilized in a matrix, $A(\infty) = 0$.

The values of the β_i and σ_i are calculated by a least-squares iterative fitting procedure, using the FIT8 program supplied by the manufacturer [16]. In this procedure the computed values of the α_i and τ_i are used to generate an impulse response function which represents $S(t)$, the time-dependent fluorescence intensity, according to eq. 2. Trial values of the β_i and σ_i are used to calculate a corresponding impulse response function for the anisotropy, $A(t)$. $A(t)$ is multiplied by $S(t)$ to yield a trial representation of the deconvoluted difference decay function, $D(t)$. $D(t)$ is convolved with the instrumental response function $P(t)$ to yield a computed difference decay function $D_{\mathrm{com}}(t)$. $D_{\mathrm{com}}(t)$ is compared with the experimental difference decay curve $D_{\mathrm{exp}}(t)$.

For each set of the trial values of the β_i and σ_i, the corresponding value of χ^2 is computed from:

$$\chi^2 = \sum_j \left\{ \frac{D_{\mathrm{com}}(j) - D_{\mathrm{exp}}(j)}{\rho(j)} \right\}^2 \tag{6}$$

where $D_{\mathrm{com}}(j)$, etc., are the values of these quantities for the j-th data point. In this case the precision $\rho(j)$ is equal to $\sqrt{V(j)}$, where $V(j)$ is the associated variance. The optimum values of the β_i and σ_i are located by an iterative procedure simi-

Table 1

Computation of decay times of fluorescence intensity assuming different models

Conditions: 100 μM calmodulin in 50 mM Mops, 5 mM Ca^{2+}, pH 6.5, 11° C, plus 50 μM TNS.

Assumed number of components	α_1	τ_1	α_2	τ_2	α_3	τ_3	χ^2_N
1	0.3832	8.53	–	–	–	–	18.99
2	0.1702	11.15	0.2626	5.30	–	–	1.99
3	0.1052	12.36	0.2943	6.48	0.1009	0.945	1.49

Table 2

Computation of rotational correlation times assuming different models

Conditions: 70.4 μM calmodulin plus 9.6 μM TNS in 50 mM potassium acetate, 4 mM Ca^{2+}, pH 5.0, 40° C.

Assumed number of rotational modes	Assumed number of components in impulse response function	β_1	σ_1 (ns)	β_2	σ_2 (ns)	χ^2_N
1	3	0.27	6.3	–	–	1.27
2	3	0.20	8.5	0.09	2.6	1.11

Table 3

Decay parameters of fluorescence intensity

System	Concentration (μM)	Solvent	pH	T	α_1	τ_1	α_2	τ_2	α_3	τ_3	$\bar{\tau}$	χ^2_N
CaM	100	50 mM Ac	5.0	12	–	–	0.21	7.9 ±0.1	0.23	16.3 ±0.1	13.7 ±0.1	1.4
CaM	105	50 mM Ac	5.0	25	–	–	0.11	6.8 ±0.1	0.08	15.8 ±0.1	12.4 ±0.1	1.5
CaM	105	50 mM Ac	5.0	40	–	–	0.24	5.9 ±0.1	0.16	14.8 ±0.1	11.4 ±0.1	1.3
CaM	113	50 mM Mops	6.5	12	0.1	0.9 ±0.1	0.29	6.5 ±0.2	0.11	12.4 ±0.1	8.8 ±0.2	1.5
CaM	142	50 mM Mops	6.5	25	0.05	1.9	0.22	6.9 ±0.1	0.06	14.3 ±0.1	9.2 ±0.1	1.3
CaM	142	50 mM Mops	6.5	40	0.10	1.4	0.32	6.2 ±0.1	0.09	13.3 ±0.1	8.6 ±0.1	1.2
CaM	141	50 mM Mops, 2 M KCl	6.5	25	0.09	4.0 ±0.1	0.14	9.0 ±0.1	0.02	17.8 ±0.1	9.4 ±0.1	1.3
CaM	125	0.1 M Tris	9.0	25	–	–	0.28	4.7 ±0.1	0.13	9.5 ±0.1	7.0 ±0.1	1.7
CaM	278	50 mM $NaHCO_3$	9.5	25	0.07	1.3	0.17	5.6 ±0.1	0.01	9.6 ±0.1	5.4 ±0.1	1.0
CaM + ME (28)	22	50 mM Mops	6.5	12	–	–	0.04	6.1 ±0.2	0.23	12.3 ±1.1	11.8 ±1.0	1.6
CaM + ME (28)	22	50 mM Mops	6.5	25	–	–	0.21	9.0 ±0.1	0.18	13.4 ±0.3	11.5 ±0.2	1.6
TM_1	62	50 mM Mops	6.5	12	–	–	0.30	8.4 ±0.1	0.09	13.5 ±0.7	10.1 ±0.3	1.1
TM_1	62	50 mM Mops	6.5	25	–	–	0.31	8.5 ±0.1	0.08	14.0 ±0.4	10.1 ±0.2	1.0
TR_2C	58	50 mM Mops	6.5	10	0.96	0.5 ±0.1	0.18	5.0 ±0.1	0.14	11.8 ±0.1	8.1 ±0.1	1.3
TR_2C	55	50 mM Mops	6.5	25	0.20	0.7 ±0.1	0.25	4.9 ±0.1	0.15	9.2 ±0.1	6.8 ±0.1	1.7

lar to that used to determine the decay times.

In tables 1–4 normalized values of χ^2, χ^2_N, are cited. χ^2_N is equal to χ^2/F, where F is the number of degrees of freedom and is equal to the number of data points (time channels) minus the number of determined parameters.

In the programs described above, the time frame shift between exciting and emitted light may be treated as a variable or fixed at a constant value. In determining the decay times of fluorescence intensity, the time frame shift between exciting and emitted light was allowed to float and the value selected which was consistent with the optimum fit. The values were invariably less than 100 ps in magnitude. In computing the rotational correlation times the time frame shift was fixed at the same value as was used in generating the impulse response function and was equal to that obtained in the determination of the corresponding set of decay times of fluorescence intensity. The limiting anisotropy at very long times $A(\infty)$ was fixed at zero in the determination of the rotational correlation times cited here. A second determination was also made in each case, in which $A(\infty)$ was allowed to float. If the determined value was greater than 2×10^{-2}, the data were discarded.

In applying the above procedures, the time decay of fluorescence intensity was fitted assum-

Table 4

Decay parameters of fluorescence anisotropy

System [a]	Solvent	pH	T	β_1	σ_1	σ_1^{25}	β_2	σ_2	σ_2^{25}	$\bar{\sigma}^{25}$ [d]	χ^2_N	No. of determinations
CaM	50 mM Ac	5.0	12	0.24	19.0 ±2.0	13.3 ±1.4	0.05	2.5 ±0.3	1.8 ±0.2	11.3 ±1.2	1.0	2
CaM	50 mM Ac	5.0	25	0.24	12.9 ±1.4	12.9 ±1.4	0.07	2.9 ±0.9	2.9 ±0.9	10.7 ±1.2	1.0	2
CaM	50 mM Ac	5.0	40	0.19	8.9 ±2.0	12.7 ±2.8	0.09	2.2 ±0.4	3.1 ±0.6	9.6 ±2.1	1.1	2
CaM	50 mM Mops	6.5	12	0.21	15.2 ±1.5	10.6 ±1.0	0.085	2.0 ±0.5	1.4 ±0.3	7.9 ±0.8	1.0	3
CaM	50 mM Mops	6.5	25	0.18	10.5 ±1.5	10.5 ±1.5	0.09	1.5 ±0.5	1.5 ±0.5	7.5 ±1.0	1.1	4
CaM	50 mM Mops	6.5	40	0.17	7.8 ±2.2	11.3 ±3.0	0.10	1.5 ±0.5	2.2 ±0.7	7.9 ±2.2	1.0	3
CaM	50 mM Mops, 2 M KCl	6.5	25	0.19	12.1 ±2.0	12.1 ±2.0	0.10	1.9 ±0.3	1.9 ±0.3	8.6 ±1.5	1.0	2
CaM	0.1 M Tris	9.0	25	0.16	11.2 ±1.0	11.2 ±1.0	0.13	2.2 ±0.5	2.2 ±0.5	7.2 ±1.0	1.0	1
CaM	50 mM $NaHCO_3$	9.5	25	0.18	8.9 ±1.0	8.9 ±1.0	0.11	1.3 ±0.3	1.3 ±0.3	6.0 ±0.7	1.1	1
CaM +ME [b]	50 mM Mops	6.5	12	–	–	–	0.29	13.0 ±1.4	9.0 ±1.0	9.0 ±1.0	1.0	2
CaM +ME [b]	50 mM Mops	6.5	25	–	–	–	0.23	9.6 ±1.5	9.6 ±1.5	9.6 ±1.5	1.2	2
TM_1 [c]	50 mM Mops	6.5	12	0.29	9.1 ±0.1	6.3 ±0.1	0.02	1.3 ±0.8	0.9 ±0.7	6.0 ±0.1	1.0	1
TM_1 [c]	50 mM Mops	6.5	25	0.25	5.9 ±0.1	5.9 ±0.1	0.12	0.4 ±0.1	0.4 ±0.1	4.2 ±0.1	1.0	1
TR_2C [c]	50 mM Mops	6.5	10	–	–	–	0.26	9.7 ±0.4	6.5 ±0.3	6.5 ±0.3	1.3	1
TR_2C [c]	50 mM Mops	6.5	25	–	–	–	0.21	4.4 ±0.1	4.4 ±0.1	4.4 ±0.1	1.1	1

[a] The concentration of CaM ranged from 140 to 100 μM, unless otherwise stated; the TNS level was 0.1–0.5 of that of CaM.
[b] CaM, 22 μM; ME, 28 μM.
[c] 60 μM
[d] $\bar{\sigma}^{25} = \Sigma\beta_i\sigma_i^{25}/\Sigma\beta_i$.

ing one, two, and three decay times. In most cases, physically meaningful parameters were obtained for all three models, the goodness of fit, as measured by χ^2_N, increasing with the assumed number of components. In some cases the three-component fit failed, yielding a negligibly small lifetime or amplitude. Since in all such cases a two-component fit yielded a satisfactory value of χ^2_N and a random distribution of residuals, the decay parameters obtained from the two-component fits were used in subsequent calculations. A representative set of calculations of decay times is cited in table 1.

The time decay of fluorescence anisotropy was fitted using impulse response functions generated with the maximum number of intensity decay times (usually three) which could be meaningfully obtained. However, little difference in the value of χ^2_N was usually observed between two- and three-component impulse response functions. Fits were made assuming one and two correlation times. With two exceptions, physically meaningful parameters were obtained for both models, a substantial improvement in χ^2_N occurring for the assumption of two rotational modes. A typical set of calculations of correlation times is given in table 2.

In subsequent tabulations (tables 3 and 4), only the parameters corresponding to the optimum fit obtained have been cited.

Correlation times determined at a temperature other than 25°C were corrected to the standard conditions of H_2O, 25°C, by the relation

$$\sigma_{25} = \sigma_T (T/\eta)_T / (T/\eta)_{25} \qquad (7)$$

where σ_{25} and σ_T are the correlation times at 25°C and temperature T, respectively, and η is the solvent viscosity.

Separations by HPLC chromatography were made using a Perkin-Elmer HPLC apparatus.

3. Results

3.1. TNS complexes with intact calmodulin

Throughout these measurements the mole ratio of TNS to calmodulin was maintained at 0.5 or less to minimize any binding to secondary sites and to favor confinement of the bound probe to the strongest site or sites present. The dissociation constant of the TNS-calmodulin complex at neutral pH has been reported to be 10–20 μM [9,10]. For the levels of protein and TNS employed here (tables 3 and 4), 70% or more of the dye should be combined. At pH 6.5 the emission spectrum has a maximum intensity at 450 nm; at pH 5.0 the maximum is shifted to 438 nm with some increase in intensity (fig. 1). For all measurements cited here, the fluorescence of TNS alone was less than 1% of that in the presence of protein.

For all conditions studied the time decay of fluorescence intensity was multi-exponential. Two or three components were required to obtain an optimal fit of the data; the goodness of fit, as measured by χ^2_N, improved significantly as the assumed number of components increased from one to two or three. While the use of three or, in some instances, two components yielded acceptable fits of the data, as judged by both the values of χ^2_N and the distribution of residuals, this does not necessarily establish that this number of components are strictly present or rule out the ex-

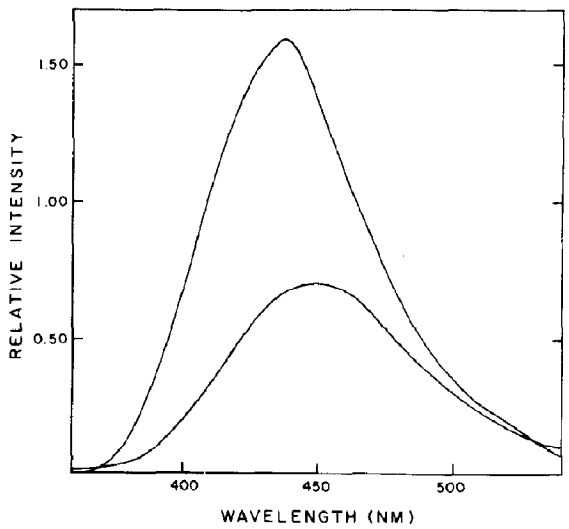

Fig. 1. Fluorescence emission spectrum for calmodulin (71 μM) plus TNS (48 μM). The excitation wavelength is 330 nm. Lower curve: 50 mM Mops, 5 mM Ca^{2+}, pH 6.5; upper curve, 50 mM Na^+ acetate, 5 mM Ca^{2+}, pH 5.0.

istence of additional components or of a continuous distribution of decay times.

In one series of experiments conditions were chosen so as to resemble those for which calmodulin was crystallized for X-ray diffraction studies, with the objective of maximizing the likelihood of obtaining a rigid molecule approximating the crystallographic structure of calmodulin [5]. For this purpose, the TNS-calmodulin complex was examined at pH 5.0 in the presence of excess Ca^{2+} (fig. 2 and tables 2 and 3). At this pH, which approaches the isoelectric point of calmodulin, intramolecular electrostatic repulsion, which tends to destabilize organized structure, should be minimal.

The time decay of fluororescence intensity at pH 5.0 was multi-exponential at each of the three temperatures examined (fig. 2 and table 3). Two

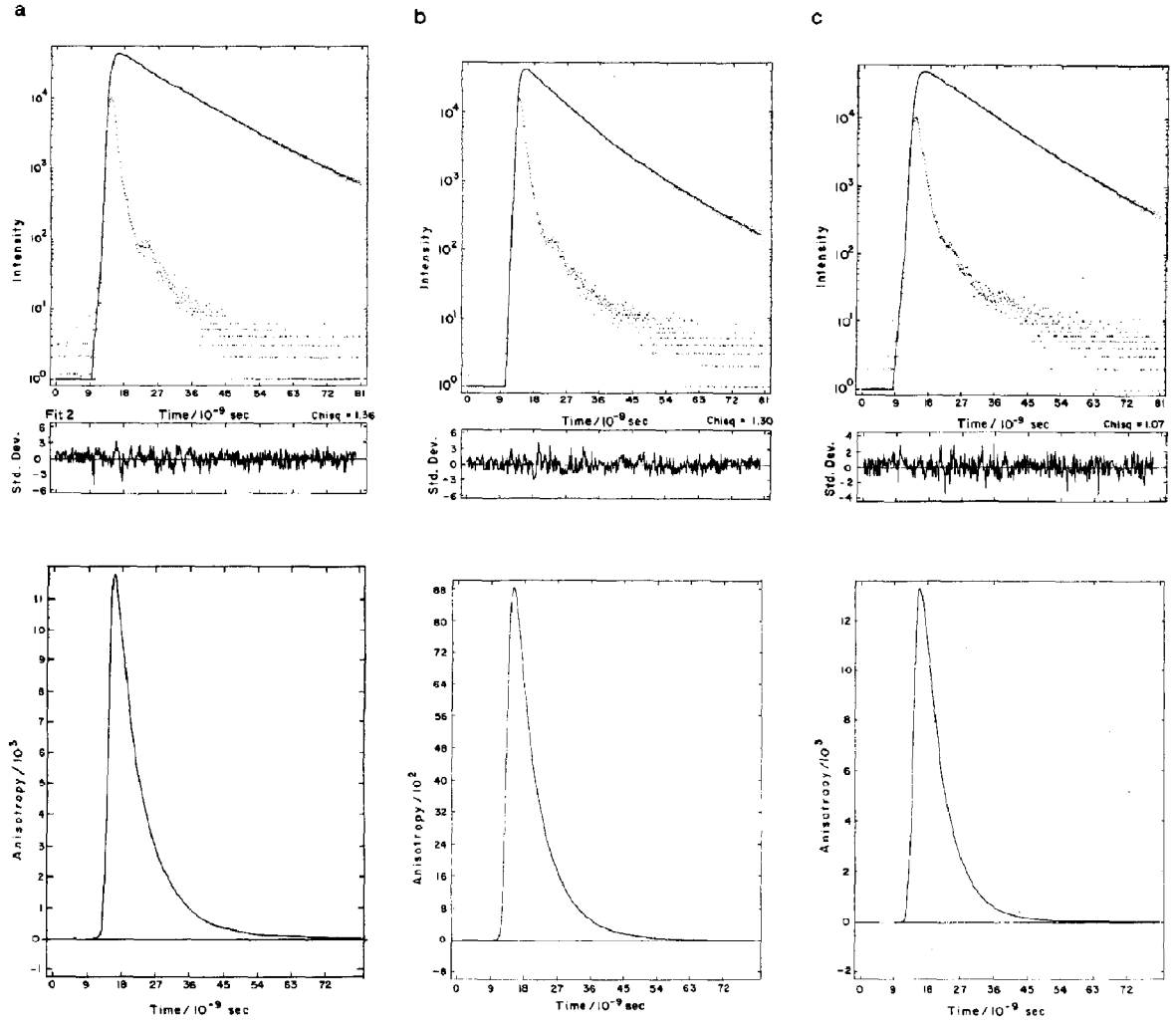

Fig. 2. (Upper curves) Comparison of the reconvolved computed curves of intensity decay with the actual data. The parameters cited in table 3 were used in each case. The residuals are shown in the lower portion. (Lower curves) Comparison of the computed and experimental curves for VV – gVH. The parameters cited in table 4 were used. (a) 50 mM Ac, 5 mM Ca^{2+}, pH 5.0, 13 °C. (b) 50 mM Mops, 5 mM Ca^{2+}, pH 6.5, 25 °C. (c) Plus melittin (107 μM), 50 mM Mops, 5 mM Ca^{2+}, pH 6.5, 25 °C.

components were sufficient to obtain an optimal fit at 12, 25 and 40 °C (table 3). Attempts to obtain a three-component fit yielded either a negative amplitude or a third component of negligibly small amplitude. The intensity-average decay time ($=\Sigma\alpha_i\tau_i^2/\Sigma\alpha_i\tau_i$) decreased significantly with increasing temperature (table 3).

The observed multiplicity of decay times could, in principle, arise from a heterogeneity of binding sites. However, results with the TR_2C fragment, which will be discussed subsequently, make this unlikely. A more likely explanation is the sampling of different microenvironments by the probe as a consequence of its localized motion, or else relaxation processes involving the solvent or adjacent residues on the protein surface.

The time decay of fluorescence anisotropy at pH 5.0 was also multi-exponential at all three temperatures and could be adequately fitted in terms of two rotational modes with different correlation times (fig. 2 and table 4). The longer of these, which has a magnitude of 13.0 ± 1.5 ns when corrected to the standard conditions of H_2O, 25 °C, clearly represents the rotational motion of a major portion of the calmodulin molecule. The shorter correlation time, whose magnitude corrected to standard conditions is 2–3 ns, must correspond to the motion of some structural subelement. The corrected magnitude of the shorter correlation time shows some upward drift with increasing temperature. This may reflect the inadequacy of eq. 7 when applied to a correlation time influenced by internal rotations which do not respond in the standard way to a change in bulk viscosity.

At pH 5.0 the amplitudes of the two rotational modes, as well as the magnitudes of the corresponding correlation times, do not vary greatly with temperature over the range 5–40 °C, apart from a minor decrease in the amplitude, β_1, corresponding to the longer correlation time at 40 °C. At all temperatures the anisotropy decay is dominated by the slower rotational mode.

An interpretation of these results in terms of the structure of calmodulin will be deferred to section 4.

The behavior of TNS-calmodulin complexes at pH 6.5 qualitatively resembles that observed at pH 5.0, but some quantitative differences exist. In this case three components were required for an optimal fit of the time decay of fluorescence intensity at all three temperatures (fig. 2 and table 3).

The time decay of fluorescence anisotropy is likewise multi-exponential (fig. 2 and table 4) and can be fitted in terms of a longer correlation time ($\sigma_1^{25} \simeq 10.5 \pm 1.5$ ns), which reflects the motion of a major portion of the molecule, and a shorter correlation time ($\sigma_2^{25} \simeq 2$ ns), which corresponds to a more localized motion. The relative value of β_1 is substantially less at 40 °C than at the two lower temperatures. This observation is consistent with, and suggests, that the probe senses a higher rotational mobility with increasing temperature. However, the value of β_1/β_2 at 11 °C is less at pH 6.5 than at pH 5.0, suggesting that the more rapid rotational mode is more prominent at the former pH. The presence of 2 M KCl at pH 6.5 results in little change other than a slight increase in the values of the individual decay times of fluorescence intensity (table 3). The time decay of anisotropy required two components for a satisfactory fit; the magnitude of the longer correlation time is similar to the value found in the absence of KCl (table 4).

An increase in pH to the more alkaline value of 9.0 results in a decrease in the magnitudes of the individual decay times, as well as that of the average decay time (table 3). The relative amplitude corresponding to the longer correlation time characterizing the time decay of anisotropy is significantly reduced from the value at pH 6.5 (table 4). A further increase in pH to 9.5 results in a further decrease in the amplitude associated with the longer correlation time, as well as the average correlation time ($\bar{\sigma}^{25}$) (table 4). This result is suggestive of an increase in the rotational mobility sensed by the probe at alkaline pH, presumably reflecting some loss of organized structure.

3.2. TNS complexes with calmodulin plus melittin

The bee venom polypeptide melittin has been shown to interact with Ca^{2+}-liganded calmodulin with high affinity ($K_d < 1$ nM) to form a 1:1

complex [17,18], in which the melittin exists in a largely α-helical conformation [17–19]. There is increasing evidence that the melittin forms extensive contacts with the α-helical strand (residues 66–92) which joins the N- and C-terminal lobes and with the adjacent portion of the C-terminal lobe [19].

In the presence of excess melittin, the fluorescence intensity of bound TNS is substantially increased (fig. 3), with a shift of the emission maximum to shorter wavelengths. The implication is that either a pre-existing binding site is modified in the melittin-calmodulin complex, or else a new site is developed with altered characteristics. The time decay of fluorescence intensity could be fitted adequately in terms of two decay times (table 3 and fig. 2) which were comparable in magnitude to those for native calmodulin. In view of the similarity in average decay time it is unlikely that the increased fluorescence intensity arises from a higher quantum yield of bound TNS.

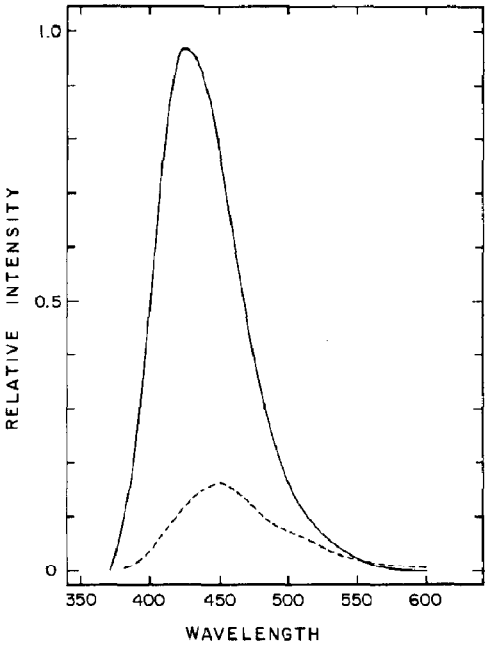

Fig. 3. Fluorescence emission spectrum of calmodulin (58 μM) plus TNS (1.9 μM) in the absence and presence of melittin (74 μM). Solvent: 50 mM Mops, 5 mM Ca^{2+}, pH 6.5, (lower curve), no melittin; (upper curve) melittin present.

It is more probable that it reflects an enhanced binding of TNS by the complex, although actual binding data are not available.

It is of particular interest that the anisotropy decay could be acceptably fitted with the assumption of a single rotational mode (table 4) at both 12 and 25° C. Attempts to obtain two-component fits were unsuccesful, leading either to a negligibly short correlation time or else to two decay times of equivalent magnitude. Apparently, the localized mobility of the TNS probe which is detected for other conditions is suppressed by formation of the melittin complex, so that the probe is now almost immobilized with respect to the protein matrix.

A surprising finding is that the magnitude of the single observed correlation time is slightly reduced from that of the longer correlation time for native calmodulin, although the molecular weight of the complex is increased by 15%. Consideration of this point will be deferred to section 4.

3.3. TNS complexes with calmodulin fragments

The time decay of fluorescence intensity for complexes of TNS with the TR_2C (78–148) fragment produced by trypsin digestion was multi-exponential at both 10 and 25° C, requiring the assumption of three components for an acceptable fit (table 3). It is of interest that the multi-exponential decay persists for this fragment, since it possesses only a single binding site for TNS [9]. This reinforces the view that the multicomponent decay does not arise from a heterogeneity of binding sites but rather from the interaction of the probe with its microenvironment. It is of interest that the magnitudes of the individual decay times are rather similar to those observed for native calmodulin under the same conditions.

An unexpected feature of the time decay of fluorescence anisotropy was the detection of only a single rotational mode at both 10 and 25° C. In both cases a one-component fit yielded an acceptable value of χ^2_N, while attempts at a two-component fit resulted in negative amplitudes for one component. The magnitude of the single correlation time observed at 10° C was roughly half that of the longer correlation time detected for

native calmodulin under these conditions.

In contrast to TR_2C, the TM_1 (1–106) fragment produced by thrombin digestion, which contains an intact connecting bridge, shows a multicomponent time decay of anisotropy, which can be fitted adequately in terms of two rotational modes (table 4). The longer correlation time is intermediate in magnitude to those for TR_2C and native calmodulin.

4. Discussion

The crystallographic structure of Ca^{2+}-liganded calmodulin is significantly elongated and asymmetric and if it persisted in solution, would be expected to display an average rotational correlation time which is elevated over the value predicted for a sphere of the same molecular weight. In comparing observed with predicted correlation times, it is necessary to assume a hydrodynamic model for the molecule. The conventional approach is to approximate the actual, somewhat irregular shape, by a smooth ellipsoid of revolution [20].

The crystallographic structure is about 65 Å long, while the N- and C-terminal lobes are about 20 Å in diameter. The diameter of the connecting helical strand may be estimated to average 8–10 Å, if side chains are included. Thus, if the molecule is approximated by a prolate ellipsoid of revolution, its average axial ratio should be ~ 4. Alternatively, the axial ratio of the equivalent ellipsoid with the same length and volume is 2.6. The effective axial ratio is probably not far from 3.0.

Belford et al. [21] have developed a general theory for the time decay of fluorescence anisotropy for a rigid ellipsoidal particle in which internal rotations are absent. For the case of a symmetrical ellipsoid of revolution, their equation becomes:

$$A(t) = \beta_1 e^{-t/\sigma_1} + \beta_2 e^{-t/\sigma_2} + \beta_3 e^{-t/\sigma_3} \qquad (8)$$

where

$$\sigma_1 = 1/6D_2$$

$$\sigma_2 = 1/(5D_2 + D_1)$$

$$\sigma_3 = 1(2D_2 + 4D_1)$$

and

$$\beta_1 = 0.1(3\cos^2\theta_1 - 1)(3\cos^2\theta_2 - 1)$$

$$\beta_2 = 0.3 \sin 2\theta_1 \sin 2\theta_2 \cos\phi$$

$$\beta_3 = 0.3 \sin^2\theta_1 \sin^2\theta_2(\cos^2\phi - \sin^2\phi)$$

Here D_1 and D_2 are the rotary diffusion coefficients for rotation about either equatorial axis and about the long axis, respectively; θ_1 and θ_2 are the angles formed by the absorption and emission transition moments with the axis of symmetry of the ellipsoid and ϕ is the angle formed by the projection of the two moments in the plane perpendicular to the axis of symmetry.

For an ellipsoid of revolution, the values of D_1 and D_2 are related to the axial ratio, γ, and the rotary diffusion coefficient of the equivalent sphere, D_0, by:

$$D_1/D_0 = \frac{3}{2}\frac{\gamma(\gamma - \epsilon)}{(\gamma^2 - 1)} \qquad (9)$$

$$D_2/D_0 = \tfrac{3}{2}\gamma\frac{[(2\gamma^2 - 1)\epsilon - \gamma]}{(\gamma^4 - 1)}$$

where $\epsilon = (\gamma^2 - 1)^{-1/2} \ln[\gamma + (\gamma^2 - 1)^{1/2}]$. D_0 is given by:

$$D_0 = kT/6\eta V$$

where k is the Boltzmann constant, T the absolute temperature, η the solvent viscosity, and V the molecular volume. The value of V is equal to the anhydrous volume plus an increment reflecting the bound water of hydration. Computed values of σ_1, σ_2, and σ_3 are cited in table 5 as a function of axial ratio and hydration.

If the shape of Ca^{2+}-liganded calmodulin is approximated by a rigid prolate ellipsoid of revolution, three special cases are of interest:

(a) The direction of the absorption transition moment is that of the axis of symmetry. In this case, $\beta_2 = \beta_3 = 0$ and the only correlation time observed is σ_1.

(b) The transition moments of absorption and emission lie in the plane perpendicular to the axis of symmetry. In this case,

$$\beta_1 = 0.1$$

$$B_2 = 0$$

Table 5

Computed values of correlation times

Axial ratio	Hydration	σ_1	σ_2	σ_3	σ_h^a
1.0	0	4.4	4.4	4.4	4.4
2.0	0	6.6	5.8	4.4	5.4
3.0	0	10.2	7.5	4.4	6.5
4.0	0	14.9	9.2	4.4	7.4
1.0	0.2	5.6	5.6	5.6	5.6
2.0	0.2	8.4	7.4	5.6	6.9
3.0	0.2	13.0	9.6	5.6	8.3
4.0	0.2	19.0	11.7	5.6	9.5

[a] Harmonic mean correlation time.

$$\beta_3 = 0.3(2\cos^2\lambda - 1)$$

where $\lambda = \phi$ = angle between the two transition moments.

(c) The transition moments of absorption and emission are randomly oriented with respect to the axes of the molecule. In this case,

$$\beta_1 = (3\cos^2\lambda - 1)/25$$

$$\beta_2 = \beta_3 = 2(3\cos^2\lambda - 1)/25$$

Considering first the results for native calmodulin at pH 6.5 and 5.0, a comparison with the computed values in table 5 indicates that in no case are the observations in complete accord with the predictions for a rigid ellipsoid. In particular, the magnitude of the shorter correlation time is substantially less than the smallest value predicted for axial ratios of 3 or 4 and probably arises from some form of internal rotation.

At pH 5.0 and 6.5 the magnitude of the longer correlation time is 11–13 ns. This is close to the value expected for σ_1 for an axial ratio of 3.0 and a hydration of 0.2. A model consistent with these results is one in which the bound TNS senses the rotation of the entire molecule and the axes of absorption and emission are approximately parallel to the long axis, corresponding to case (a) cited above.

Superimposed upon the motion of the entire molecule is a more localized rotation of the probe with a correlation time of 2–3 ns. The magnitude of this correlation time is such as to suggest that it does not arise from rotation confined to the probe, but rather from that of a group of residues in proximity to the binding site. The noncovalent attachment of TNS, which presumably involves contact with several amino acid side chains, lends plausibility to this model.

While the magnitudes of both correlation times are similar at pH 6.5 and 5.0, there is a significant difference in the relative amplitude of the two rotational modes for these conditions, the relative amplitude of the more rapid rotational mode being substantially less at the latter pH. This is suggestive of a partial loss of localized flexibility in the vicinity of the binding site and of a more rigid conformation.

The formation of a 1 : 1 complex with melittin results in the loss of the more rapid rotational mode. There is now substantial evidence that the combined melittin exists in the complex largely in an α-helical conformation which extends along the connecting bridge and onto the neighboring portion of the C-terminal lobe [17–19]. It is not surprising that such a complex would be more rigid than native calmodulin.

The correlation time of the CaM-melittin complex is actually reduced from that of calmodulin, despite a 15% increase in molecular weight. This can be readily accounted for in terms of an altered orientation of the transition moments with respect to the axes of the particle, so that they are no longer parallel to the long axis. The observed correlation time of approx. 9 ns is in the range expected for the harmonic mean of the three characteristic correlation times of the equivalent ellipsoid of axial ratio 3, and probably corresponds to an average value. The three theoretically predicted correlation times are not sufficiently different in magnitude to be readily resolved by this type of measurement.

The magnitude of the single correlation time observed for the TR_2C fragment at 10°C is approximately half that of the longer correlation time for native calmodulin under the same conditions. As the mass of the fragment is half that of native calmodulin this is consistent with the model presented above, which attributes the slower rotational mode to the motion of the entire molecule, provided that the orientation of the transition

dipoles is similar for the two cases. There is no very obvious explanation for the absence of the more rapid rotational mode in this case. Since it is present for the TM_1 fragment, which has an intact connecting bridge, it may be associated with the persistence of this structural feature, perhaps reflecting a bending or twisting motion of the bridge. Scission of the bridge with possibly some degree of unwinding from the new terminus might result in this rotational mode becoming too rapid to be readily detected.

5. Conclusions

(1) Time domain fluorescence anisotropy measurements upon TNS-liganded calmodulin are consistent with the crystallographic structure.

(2) An internal rotational mode exists which becomes more important at pH 6.5 than at pH 5.0.

References

1 W.Y. Cheung, Science 207 (1980) 19.
2 C.B. Klee, T.H. Crouch and P.G. Richman, Annu. Rev. Biochem. 49 (1980) 489.
3 R.H. Kretsinger, CRC Crit. Rev. Biochem. 8 (1980) 119.
4 P.K. Lambooy, R.F. Steiner, and H. Sternberg, Arch. Biochem. Biophys. 217 (1982) 517.
5 Y.S. Babu, J.S. Sack, T.G. Greenbough, C.E. Bugg, A.R. Means and W.J. Cook, Nature 315 (1985) 37.
6 H. Sternberg and R.F. Steiner, Biopolymers 21 (1982) 1411.
7 R.F. Steiner, P.K. Lambooy and H. Sternberg, Arch. Biochem. Biophys. 222 (1983) 204.
8 T. Tanaka and H. Hidaka, J. Biol. Chem. 255 (1980) 962.
9 J. Suko, J. Pidlich and O. Bertel, Eur. J. Biochem. 153 (1985) 451.
10 A. Follenius and D. Gerard, Biochem. Biophys. Res. Commun. 119 (1984) 1154.
11 D.C. Dalgarno, R.E. Klevitt, B.A. Levine, G.M.M. Scott, R.J.P. Williams, J. Gergely, Z. Grabarek, P.C. Leavis, R.J.A. Grand and W. Drabikowski, Biochim. Biophys. Acta 791 (1984) 164.
12 D.M. Watterson, F. Sharief and T.C. Vanaman, J. Biol. Chem. 255 (1980) 962.
13 H. Brzeska, J. Szynkiewicz and W. Drabikoroski, Biochem. Biophys. Res. Commun. 115 (1983) 87.
14 D. Guerini, J. Krebes and E. Carafoli, J. Biol. Chem. 259 (1984) 15172.
15 D.L. Newton, M.D. Oldwurtel, M.H. Krinks, J. Shiloach and C.B. Klee, J. Biol. Chem. 259 (1983) 4419.
16 M.D. Barkley, A.A. Kowalczyk and L. Brand, J. Chem. Phys. 75 (1981) 3581.
17 M. Comte, Y. Maulet and J.A. Cox, Biochem. J. 209 (1983) 269.
18 Y. Maulet and J.A. Cox, Biochemistry 22 (1983) 5680.
19 R.F. Steiner, L. Marshall and D. Needleman, Arch. Biochem. Biophys. 246 (1986) 286.
20 C.R. Cantor and P.R. Schimmel, Biophysical chemistry,vol. 2 (Freeman, San Francisco, 1980).
21 C.G. Belford, R.L. Belford and G. Weber, Proc. Natl. Acad. Sci. U.S.A. 69 (1972) 1392.
22 L. Stryer, J. Mol. Biol. 13 (1965) 483.
23 R.F. Steiner, Arch Biochem. Biophys. 1 (1984) 105.